

Radiative $B \rightarrow K_1$ decays in the light-cone sum rules

Jong-Phil Lee*

Korea Institute for Advanced Study, Seoul 130-722, Korea

Abstract

The weak form factor for $B \rightarrow K_{1B}$ where K_{1B} is the 1P_1 state is calculated in the light-cone sum rules (LCSR). Combining the quark model result for the form factor of $B \rightarrow K_{1A}$ with K_{1A} being the 3P_1 state, we have larger values for $B \rightarrow K_1$ form factors than the previous LCSR results. The increased form factors reduce the discrepancy between theory and the experimental data for $B \rightarrow K_1\gamma$. Some phenomenological meanings are also discussed.

PACS numbers: 12.38.Lg, 13.20.He

arXiv:hep-ph/0608087v1 8 Aug 2006

*Electronic address: jplee@kias.re.kr

I. INTRODUCTION

Radiative B decays to K are a rich laboratory for the standard model and new physics. Especially, $B \rightarrow K^*\gamma$ is well understood theoretically via $b \rightarrow s\gamma$ transition as well as experimentally. Recently, higher resonant kaons are observed by CLEO and B factories [1]. For example, BELLE collaboration has measured the radiative $B \rightarrow K_1$ decays for the first time [2]:

$$\begin{aligned}\mathcal{B}(B^+ \rightarrow K_1^+(1270)\gamma) &= (4.28 \pm 0.94 \pm 0.43) \times 10^{-5}, \\ \mathcal{B}(B^+ \rightarrow K_1^+(1400)\gamma) &< 1.44 \times 10^{-5},\end{aligned}\tag{1}$$

where K_1 is the orbitally excited axial vector meson. In the theoretical side, recent developments of the QCD factorization (QCDF) [3] makes it possible to calculate the hard spectator contributions systematically in a factorized form through the convolution at the heavy quark limit. $B \rightarrow K^*\gamma$ is already studied in this line [4, 5, 6, 7]. One good point about K_1 is that there are lots of things shared with $B \rightarrow K^*\gamma$. Basically both of them are governed by $b \rightarrow s\gamma$. And the distribution amplitudes (DA) of K^* and K_1 are same except the overall factor of γ_5 which makes few differences in many calculations.

A straightforward extension of the analysis for $B \rightarrow K^*\gamma$ to $B \rightarrow K_1\gamma$ was given in [8]. But the BELLE measurements of Eq. (2) reveal that theory predicts much smaller branching ratio than data [9, 10]. This is an opposite situation to that of $B \rightarrow K^*\gamma$ where theory predicts larger branching ratio. Considering the resemblance between K^* and K_1 , it is quite unlikely that the same theoretical framework would produce discrepancies with experiment in a reversed way.

In the previous analysis the main uncertainty of theory lies in the nonperturbative form factors. Ref. [8] relies on the light-cone sum rule (LCSR) results for the $B \rightarrow K_1$ form factors [11]. In [11] only the leading twist DAs are considered without any non-asymptotic contributions. In this paper we revisit the $B \rightarrow K_1$ form factors in the LCSR. There are three improvements compared to [11]. First, higher twist DAs are included; second, non-asymptotic contributions are also considered; third, terms proportional to m_A^2 , where m_A is the mass of axial meson, are not neglected.

For $B \rightarrow K^*$ form factors, the LCSR results are updated [12] up to the one-loop corrections to twist-2,3 contributions and leading order twist-4. It is thus legitimate to improve

the theoretical accuracy for $B \rightarrow K_1$ form factors.

It is believed that the physical $K_1(1270)$ and $K_1(1400)$ states are the mixtures of angular momentum eigenstates $^1P_1 (K_{1B})$ and $^3P_1 (K_{1A})$. The mixing angle is not known precisely, but is close to the maximal. This is a very natural and convenient way to explain the suppression of one decay mode compared to the other. For the suggestive angles $\theta = \pm 37^\circ, \pm 58^\circ$ [13], negative ones are disfavored by (2).

In [14], some of the Gegenbauer moments of K_{1B} DAs are calculated by LCSR. With this information, we explicitly calculate the $B \rightarrow K_{1B}$ form factor in LCSR. Since K_{1B} and K_{1A} have different G-parity, their Gegenbauer expansion will not be the same. Future study on K_{1A} is necessary to reinforce the reliability of current work. We use the results from model calculations for K_{1A} to give $B \rightarrow K_1$ form factors. This form factor will also be available for nonleptonic decay modes [15]

The paper is organized as follows. In the next section the weak form factors and axial vector meson DAs are defined. The LCSR evaluation is given in Sec. III. Section IV deals with the LCSR results. In Sec. V, some discussions about the results and their meanings appear. Conclusions are also added at the end of this section.

II. FORM FACTORS AND DISTRIBUTION AMPLITUDES

For the axial vector $A(p_A, \epsilon)$, where $p_A (\epsilon)$ is the momentum (polarization) of A , the relevant $B \rightarrow A$ transition matrix elements are defined as [8, 16]

$$\langle A(p_A, \epsilon) | \bar{q} i \sigma_{\mu\nu} q^\nu b | B(p_B) \rangle \quad (2)$$

$$\begin{aligned} &= F_+^A(q^2) [(\epsilon^* \cdot q)(p_B + p_A)_\mu - \epsilon_\mu^*(m_B^2 - m_A^2)] + F_-^A(q^2) [(\epsilon^* \cdot q)q_\mu - \epsilon_\mu^* q^2] \\ &\quad + \frac{F_0^A(q^2)}{m_B m_A} (\epsilon^* \cdot q) [(m_B^2 - m_A^2)q_\mu - (p_B + p_A)q^2] , \\ \langle A(p_A, \epsilon) | \bar{q} i \sigma_{\mu\nu} \gamma_5 q^\nu b | B(p_B) \rangle &= -i F_+^A(q^2) \epsilon_{\mu\nu\alpha\beta} \epsilon^{*\nu} q^\alpha (p_A + p_B)^\beta , \end{aligned} \quad (3)$$

where $q = p_B - p_A$ and $m_B(m_A)$ is the B (axial vector) meson mass. We use $\epsilon_{0123} = +1$.

The distribution amplitudes (DA) of the axial vector meson are given by [14, 17, 18]

$$\begin{aligned} & \langle A(p_A, \epsilon) | \bar{q}_1(y) \gamma_\mu \gamma_5 q_2(x) | 0 \rangle \\ &= i f_A m_A \int_0^1 du e^{i(upy + \bar{u}px)} \left\{ \frac{\epsilon^* \cdot z}{p \cdot z} p_\mu^A \left[\phi_{\parallel}(u) - g_{\perp}^{(v)}(u) \right] + \epsilon_\mu^* g_{\perp}^{(v)}(u) \right. \\ & \quad \left. + \frac{\epsilon^* \cdot z}{2(p \cdot z)^2} m_A^2 z_\mu \left[-\phi_{\parallel}(u) + 2g_{\perp}^{(v)}(u) - g_3(u) \right] \right\} , \end{aligned} \quad (4)$$

$$\langle A(p_A, \epsilon) | \bar{q}_1(y) \gamma_\mu q_2(x) | 0 \rangle = -i f_A m_A \epsilon_{\mu\nu\alpha\beta} \epsilon^{*\nu} p^\alpha z^\beta \int_0^1 du e^{i(upy + \bar{u}px)} \frac{1}{4} g_{\perp}^{(a)}(u) , \quad (5)$$

$$\begin{aligned} & \langle A(p_A, \epsilon) | \bar{q}_1(y) \sigma_{\mu\nu} \gamma_5 q_2(x) | 0 \rangle \\ &= f_A^\perp \int_0^1 du e^{i(upy + \bar{u}px)} \left\{ (\epsilon_\mu^* p_\nu^A - \epsilon_\nu^* p_\mu^A) \phi_{\perp}(u) \right. \\ & \quad + \frac{\epsilon^* \cdot z}{(p \cdot z)^2} m_A^2 (p_\mu^A z_\nu - p_\nu^A z_\mu) \left[-\frac{1}{2} \phi_{\perp}(u) + h_{\parallel}^{(t)}(u) - \frac{1}{2} h_3(u) \right] \\ & \quad \left. + \frac{m_A^2}{2p \cdot z} (\epsilon_\mu^* z_\nu - \epsilon_\nu^* z_\mu) [-\phi_{\perp}(u) + h_3(u)] \right\} , \end{aligned} \quad (6)$$

$$\langle A(p_A, \epsilon) | \bar{q}_1(y) \gamma_5 q_2(x) | 0 \rangle = f_A^\perp m_A^2 (\epsilon^* \cdot z) \int_0^1 du e^{i(upy + \bar{u}px)} \frac{1}{2} h_{\parallel}^{(s)}(u) . \quad (7)$$

Here $z = y - x$ and

$$p^\mu = p_A^\mu - \frac{m_A^2 z_\mu}{2p_A \cdot z} , \quad (8)$$

is the light-like vector, and $\bar{u} = 1 - u$. The DAs ϕ_{\parallel} (twist-2), $g_{\perp}^{(v)}$, $g_{\perp}^{(a)}$ (twist-3), and g_3 (twist-4) are anti-symmetric under the change $u \rightarrow \bar{u}$ while ϕ_{\perp} (twist-2), $h_{\parallel}^{(t)}$, $h_{\parallel}^{(s)}$ (twist-3), and h_3 (twist-4) are symmetric in $SU(3)$ limit, because of the G-parity. Thus

$$\int_0^1 du f(u) = 0 , \quad \text{for } f = \phi_{\parallel}, g_{\perp}^{(a)}, g_{\perp}^{(v)}, g_3. \quad (9)$$

The leading twist DAs are expanded with the Gegenbauer polynomials. In general, we can expand

$$\begin{aligned} \phi_{\parallel}(u) &= 6u\bar{u} \sum_{l=0}^{\infty} a_l^{\parallel} C_l^{3/2}(u - \bar{u}) , \\ \phi_{\perp}(u) &= 6u\bar{u} \left[1 + \sum_{l=0}^{\infty} a_l^{\perp} C_l^{3/2}(u - \bar{u}) \right] . \end{aligned} \quad (10)$$

For twist-3 DAs, the Wandzura-Wilczek type approximation will be used;

$$\begin{aligned}
g_{\perp}^{(v)}(u) &\simeq \frac{1}{2} \left[\int_0^u dv \frac{\phi_{\parallel}(v)}{\bar{v}} + \int_u^1 dv \frac{\phi_{\parallel}(v)}{v} \right], \\
g_{\perp}^{(a)}(u) &\simeq 2 \left[\bar{u} \int_0^u dv \frac{\phi_{\parallel}(v)}{\bar{v}} + u \int_u^1 dv \frac{\phi_{\parallel}(v)}{v} \right], \\
h_{\parallel}^{(t)} &\simeq (u - \bar{u}) \left[\int_0^u dv \frac{\phi_{\perp}(v)}{\bar{v}} - \int_u^1 dv \frac{\phi_{\perp}(v)}{v} \right], \\
h_{\parallel}^{(s)} &\simeq 2 \left[\bar{u} \int_0^u dv \frac{\phi_{\perp}(v)}{\bar{v}} + u \int_u^1 dv \frac{\phi_{\perp}(v)}{v} \right].
\end{aligned} \tag{11}$$

The twist-4 DAs will not be considered afterwards. The first few Gegenbauer coefficients are recently calculated by QCD sum rules [14].

III. SUM RULE EVALUATION

The main point of LCSR is to evaluate the two point correlation function:

$$\Pi_A = i \int d^4x e^{-ip_B \cdot x} \langle A(p_A, \epsilon) | T \left[J(0) j_B^{\dagger}(x) \right] | 0 \rangle. \tag{12}$$

Here $j_B^{\dagger}(x) = \bar{b}(x) i \gamma_5 q(x)$ is the interpolating current for B meson, and $J(y) = \bar{q}(y) \Gamma b(y)$ is the heavy-to-light current with Γ being an appropriate gamma matrices. To establish the sum rule, one calculates Π_A in two ways. On one hand, Π_A is described in terms of hadronic observables. We call this Π_A^{had} . Explicitly,

$$\Pi_A^{\text{had}} = \frac{\langle A | J(0) | B \rangle \langle B | j_B^{\dagger}(0) | 0 \rangle}{m_B^2 - p_B^2 + i\epsilon} + (\text{res.}), \tag{13}$$

where the first term is the B meson contribution and (res.) is the higher resonance one. The term $\langle A | J(0) | B \rangle$ defines the transition form factor while

$$\langle B | \bar{b} i \gamma_5 q | 0 \rangle = \frac{m_B^2}{m_b} f_B, \tag{14}$$

is proportional to the B meson decay constant f_B . Here Π_A^{had} is considered as an analytic function of p_B^2 . Using the dispersion relation,

$$\Pi_A^{\text{had}} = \int_{m_b^2}^{\infty} ds \frac{\rho^{\text{had}}(s)}{s - p_B^2}, \tag{15}$$

where $\rho^{\text{had}}(s)$ is the spectral density function. This is another expression of Eq. (13), from which we can extract the form of ρ^{had} .

On the other hand, Π_A can be written by quarks and gluons, and hence by light-cone distribution amplitudes (LCDAs). We call this Π^{LC} . From the dispersion relation,

$$\begin{aligned}\Pi_A^{\text{LC}} &= \int_{m_b^2}^{\infty} ds \frac{\rho^{\text{LC}}(s)}{s - p_B^2} \\ &= \frac{1}{\pi} \int_{m_b^2}^{\infty} ds \frac{\text{Im}\Pi_A^{\text{LC}}(s)}{s - p_B^2},\end{aligned}\quad (16)$$

where the imaginary part of Π_A^{LC} will be expressed by the LCDAs. At this stage, one assumes the quark-hadron duality for (res.) in Eq. (13) as

$$(\text{res.}) = \frac{1}{\pi} ds \int_{s_0}^{\infty} \frac{\text{Im}\Pi_A^{\text{LC}}(s)}{s - p_B^2}, \quad (17)$$

up to possible subtractions. Here s_0 is the continuum threshold from which higher multi-particle states begin. In the numerical analysis, s_0 is considered as a hadronic parameter.

Combining all this, one arrives at

$$\frac{\langle A|J(0)|B\rangle\langle B|j_B^\dagger(0)|0\rangle}{m_B^2 - p_B^2} = \frac{1}{\pi} \int_{m_b^2}^{s_0} ds \frac{\text{Im}\Pi_A^{\text{LC}}(s)}{s - p_B^2}. \quad (18)$$

After the Borel transformation over p_B^2 , we have the final expression for the sum rule:

$$e^{-m_B^2/T} \langle A|J(0)|B\rangle\langle B|j_B^\dagger(0)|0\rangle = \frac{1}{\pi} \int_{m_b^2}^{s_0} ds e^{-s/T} \text{Im}\Pi_A^{\text{LC}}(s), \quad (19)$$

where T is the Borel parameter.

Among the three form factors $F_{\pm,0}^A(q^2)$, the most important one is $F_+^A(q^2 = 0)$ since only it is responsible for the radiative decay of $B \rightarrow K_1$. Also, it can be shown that $F_+^A(0) = F_-^A(0)$ [12]. To extract F_+^A , we find it convenient to choose $J(0) = \bar{q}i\sigma_{\mu\nu}\gamma_5 q^\nu b$. The left-hand-side (L.H.S.) of Eq. (19) is simply

$$(\text{L.H.S.}) = -iF_+^A(q^2)\epsilon_{\mu\nu\alpha\beta}\epsilon^{*\nu}q^\alpha(p_B + p_A)^\beta \left(\frac{m_B^2}{m_b}f_B\right) e^{-m_B^2/T}. \quad (20)$$

The right-hand-side (R.H.S.) of Eq. (19) is rather involved. After contracting the $b\bar{b}$ quarks,

$$\begin{aligned}(\text{R.H.S.}) &= \frac{1}{\pi} \int_{m_b^2}^{s_0} ds e^{-s/T} \text{Im} \int d^4x \int \frac{d^4k}{(2\pi)^4} \frac{e^{i(k-p_B)\cdot x}}{k^2 - m_b^2 + i\epsilon} \\ &\quad \times \left[-\langle A|\bar{q}(0)\sigma_{\mu\nu}q^\nu \not{k}q(x)|0\rangle + m_b \langle A|\bar{q}(0)\sigma_{\mu\nu}q^\nu q(x)|0\rangle \right].\end{aligned}\quad (21)$$

The two matrix elements in the above equation can be written, after some gamma matrix algebra, in terms of the LCDAs, Eqs. (4)-(7). In Eqs. (4)-(7), the position coordinate x can be replaced effectively by

$$x^\mu \rightarrow \frac{\partial}{i\partial(\bar{u}p)_\mu}, \quad (22)$$

which is guaranteed by the presence of $e^{i\bar{u}px}$. On the other hand, for the factor $1/p \cdot x$

$$\begin{aligned} \frac{1}{p \cdot x} \phi(u) &\rightarrow i \int_0^u dv \phi(v), \\ \frac{1}{(p \cdot x)^2} \phi(u) &\rightarrow i^2 \int_0^u dv \int_0^v dw \phi(w), \quad (\phi = \phi_\perp, g_\perp^{(a)}, g_\perp^{(v)}, g_3) \end{aligned} \quad (23)$$

where the surface terms are vanishing. In this way, one can remove x -dependence in (R.H.S.) except in the exponent. Thus the integration over x yields a delta function, $\sim \delta^4(k - p_B + \bar{u}p)$. Another delta function appears in the imaginary part of $1/(k^2 - m_B^2 + i\epsilon)$. Combining all together, one arrives at

$$\begin{aligned} &(\text{R.H.S.}) \quad (24) \\ &= -i\epsilon_{\mu\nu\alpha\beta}\epsilon^{*\nu} q^\alpha p_A^\beta \int_{m_b^2}^{s_0} ds e^{-s/T} \int_0^1 du \left\{ f_A m_A \frac{1}{4} g_\perp^{(a)}(u) \left[-2\delta_s + (-us + um_A^2 - (1 + \bar{u})q^2)\delta'_s \right] \right. \\ &\quad \left. - f_A m_A \left[\Phi_\parallel(u)\delta_s + u g_\perp^{(v)}(u)\delta_s - m_A^2 G_3(u)\delta'_s \right] + f_A^\perp m_b \left[\phi_\perp(u)\delta_s - m_A^2 H_3(u)\delta'_s \right] \right\}. \end{aligned}$$

Here we use the short-hand notation, $\delta_s \equiv \delta(s - m_b^2 - 2\bar{u}p \cdot p_B)$, and the differentiation is with respect to $\bar{u}p$. It is understood that at the final stage of calculation, $p \rightarrow p_A$. And the newly defined functions are

$$\begin{aligned} \Phi_\parallel(u) &\equiv \int_0^u dv \left[\phi_\parallel(v) - g_\perp^{(v)}(v) \right], \\ G_3(u) &\equiv \int_0^u dv \int_0^v dw \left[-\phi_\parallel(w) + 2g_\perp^{(v)}(w) - g_3(w) \right], \\ H_3(u) &\equiv \int_0^u dv \left[h_3(v) - \phi_\perp(v) \right]. \end{aligned} \quad (25)$$

Equating Eqs. (20) and (25), after a little algebra, we have the final expression for the form

hadronic information (in GeV)		Gegenbauer moments (at 1 GeV)	
m_B	5.27	a_0^\parallel	0.26
m_b	4.8	a_1^\parallel	-1.75
f_B	0.161	a_2^\parallel	0.13
m_A	1.370	a_1^\perp	-0.13
f_A	0.195	a_2^\perp	-0.02
		a_3^\perp	-0.02

TABLE I: Input values. Gegenbauer moments are from [14].

factor $F_+^A(q^2 = 0)$

$$\begin{aligned}
F_+^A(0) = & \frac{1}{2} e^{m_B^2/T} \left(\frac{m_b}{m_B^2 f_B} \right) \left\{ f_A m_A \frac{e^{-s_0/T}}{s_0 + m_A^2} \left[-\frac{s_0 - m_A^2}{4} g_\perp^{(a)}(u_0) + m_A^2 \frac{G_3(u_0)}{u_0} \right] \right. \\
& + f_A m_A \int_{u_0}^1 \frac{du}{u} \exp \left[-\frac{m_b^2 + \bar{u} m_A^2}{uT} \right] \\
& \times \left[-\frac{uT + m_b^2 + (1 - 2u)m_A^2}{4uT} g_\perp^{(a)}(u) - \Phi_\parallel(u) - u g_\perp^{(v)}(u) + \frac{m_A^2}{T} \frac{G_3(u)}{u} \right] \\
& - f_A^\perp m_b e^{-s_0/T} \frac{m_A^2}{s_0 + m_A^2} \frac{H_3(u_0)}{u_0} \\
& \left. + f_A^\perp m_b \int_{u_0}^1 \frac{du}{u} \exp \left[-\frac{m_b^2 + \bar{u} m_A^2}{uT} \right] \left[\phi_\perp(u) - \frac{m_A^2}{T} \frac{H_3(u)}{u} \right] \right\}, \quad (26)
\end{aligned}$$

where

$$u_0 \equiv \frac{m_b^2 + m_A^2}{s_0 + m_A^2}. \quad (27)$$

IV. RESULTS

In what follows, only the case where $q^2 = 0$ is considered. The basic input constants are summarized in Table IV. The LCSR involves two important parameters, the continuum threshold s_0 and the Borel parameter T . Naively thinking, the continuum threshold is roughly

$$s_0 \simeq (m_B + \bar{\Lambda})^2 = (2m_B - m_b)^2, \quad (28)$$

where $\bar{\Lambda} \equiv m_B - m_b$. Numerically,

$$s_0 \simeq (2m_B - m_b)^2 \equiv s_* \approx 33 \text{ GeV}^2, \quad (29)$$

for $m_B = 5.27$ GeV and $m_b = 4.8$ GeV is consistent with literatures [12]. We take this value as a starting point to fix s_0 .

In principle, F_+^A is independent of the unphysical Borel parameter T . But in reality there is a sum rule window of T where a physical quantity is stable. If T is too small, then the higher twist terms proportional to $1/T^n$ ($n = 1, 2, \dots$) become too large. One requires, for example,

$$\frac{(\frac{1}{T^n} \text{ terms})}{(\text{total } F_+^A)} \lesssim 30\% . \quad (30)$$

This condition imposes the lower bound of T . The number 30% might be changed, but we adopt this value here. On the other hand, if T is too large, then the contributions from the continuum states become too large. We require that

$$\frac{\frac{1}{\pi} \int_{s_0}^{\infty} ds e^{-s/T} \text{Im}\Pi(s)}{\frac{1}{\pi} \int_{m_b^2}^{\infty} ds e^{-s/T} \text{Im}\Pi(s)} \lesssim 30\% . \quad (31)$$

This constraint imposes the upper bound of T . Note that the condition of Eq. (31) is used in [12] to determine the lower bound of continuum threshold, s_0 . In this analysis, however, we start with $s_0 = s_*$ to determine the sum rule window, and then we fix s_0 from the best stability of F_+^A within the sum rule window.

From Eqs. (30) and (31) with $s_0 = s_*$, we have

$$6.8 \leq T \leq 21.7 \text{ (GeV}^2\text{)} . \quad (32)$$

This window has overlaps with that of [11], but not with that of [12] where only vector mesons are considered. As an illustration, plots of F_+^A over T for various s_0 around s_* are given in Fig. 1. To find the best value of s_0 , we impose a simple condition. We scan s_0 which minimize the value $F_+^A(T_c + 5 \text{ GeV}^2) - F_+^A(T_c - 5 \text{ GeV}^2)$, where T_c is the central value of T within the sum rule window. We find that the best value of s_0 is

$$s_b \equiv 34.3 \text{ GeV}^2 . \quad (33)$$

Plots of F_+^A for various s_0 around s_b are shown in Fig. 2. A closer look of Fig. 2 is given in Fig. 3, and 3-dimensional plot of F_+^A against s_0 and T is given in Fig. 4. From the above analysis, we get

$$F_+^A(q^2 = 0; T_c) = 0.256_{-0.0044}^{+0.0040} , \quad (34)$$

where the errors are from the variation of s_0 around s_b by $\pm 1 \text{ GeV}^2$.

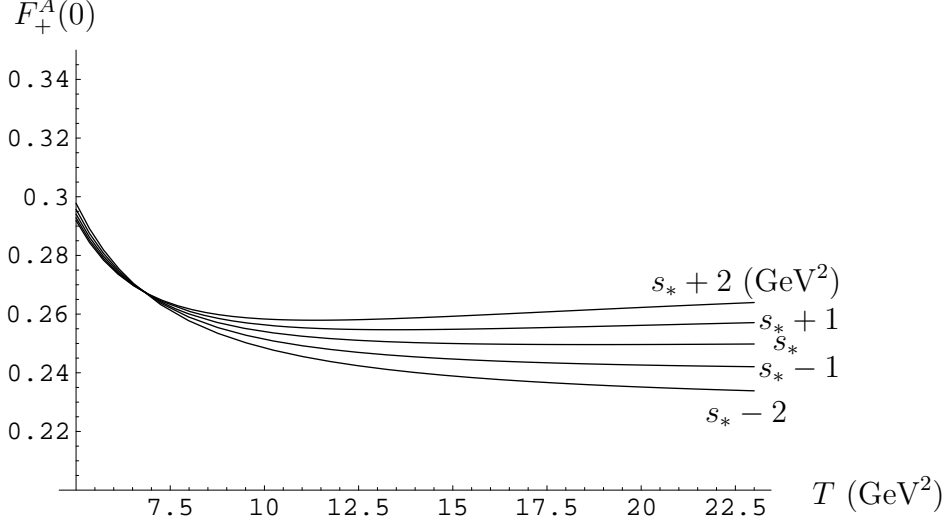


FIG. 1: $F_+^A(0)$ vs T for various s_0 around s_* .

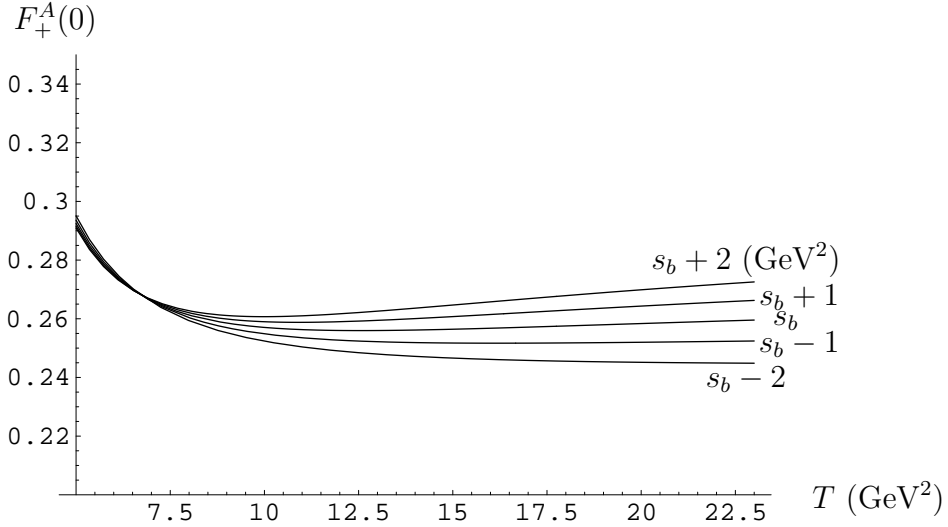


FIG. 2: $F_+^A(0)$ vs T for various s_0 around s_b .

The observed axial kaons $K_1(1270)$ and $K_1(1400)$ are mixtures of 1P_1 and 3P_1 states. Their form factors are related via mixing angle θ as [13, 19]

$$\begin{aligned} F_i^{B \rightarrow K_1(1270)} &= F_i^{A3} \sin \theta + F_i^A \cos \theta, \\ F_i^{B \rightarrow K_1(1400)} &= F_i^{A3} \cos \theta - F_i^A \sin \theta. \end{aligned} \quad (35)$$

where $i = 0, +, -$. Here, F_i^{A3} are the 3P_1 form factors. We use the result of [13], $F_+^{A3}(q^2 = 0) = 0.11$. The mixing angle θ is not yet fixed precisely. Ref. [13] suggests $\theta = \pm 37^\circ, \pm 58^\circ$. Table II shows the values of $F_+^{B \rightarrow K_1(1270)}$ and $F_+^{B \rightarrow K_1(1400)}$ for these angles. For negative

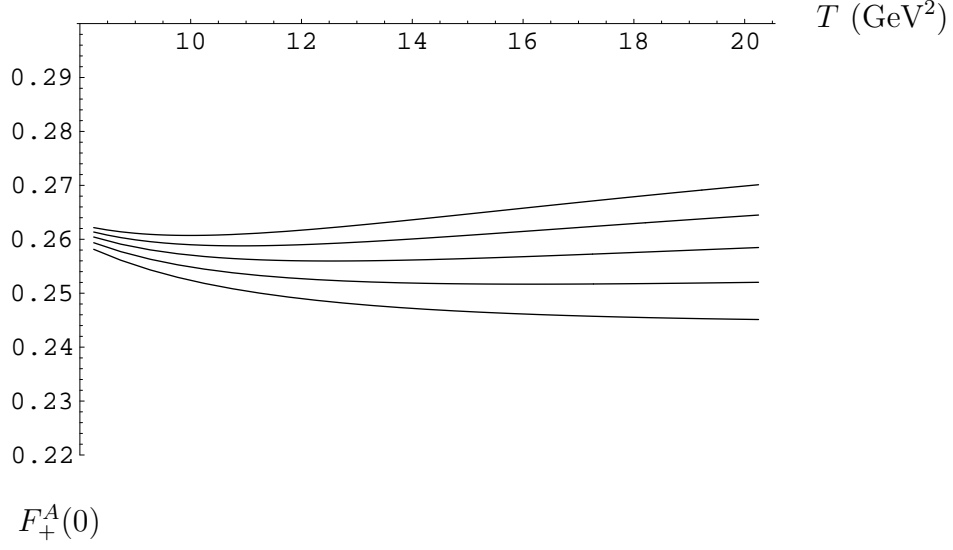


FIG. 3: A closer look of Fig. 2.

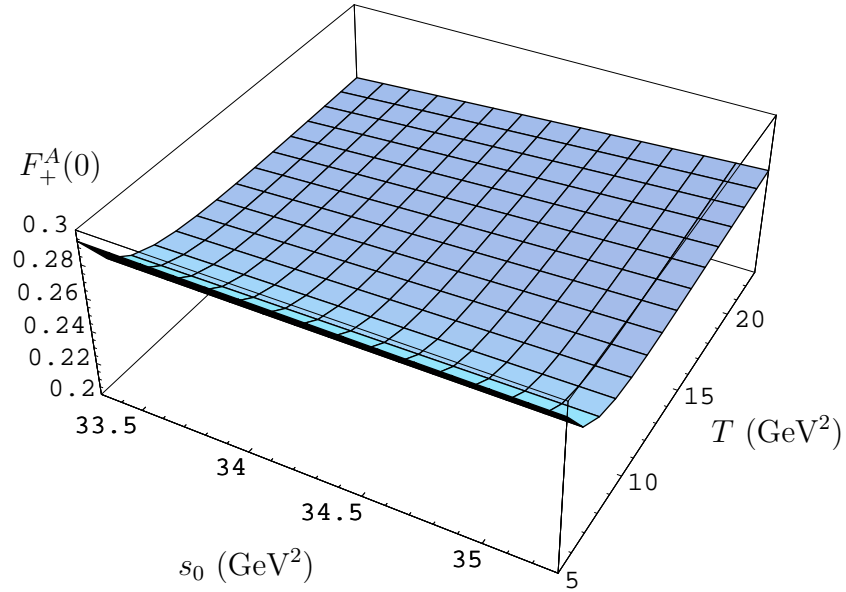


FIG. 4: 3-dimensional plot of F_+^A .

θ	37°	-37°	58°	-58°
$F_+^{B \rightarrow K_1(1270)}$	0.271	0.138	0.229	0.042
$F_+^{B \rightarrow K_1(1400)}$	-0.066	0.242	-0.159	0.276

TABLE II: $F_+^{B \rightarrow K_1(1270)}$ and $F_+^{B \rightarrow K_1(1400)}$ for various θ .

$F_{+, \text{Safir}}^A(0)$	+ (3)	+ (3)+(2)	+ (3)+(2)+(1)
0.187	0.237	0.155	0.256

TABLE III: Contributions of new improvements. The parameter set used here is the same as that in the previous section. Conditions (1), (2), and (3) are explained in the text.

angles, we find

$$F_+^{B \rightarrow K_1(1270)} < F_+^{B \rightarrow K_1(1400)} . \quad (36)$$

Since other parameters of the branching ratio are not so different in $B \rightarrow K_1(1270)\gamma$ and $B \rightarrow K_1(1400)\gamma$, one expects $\mathcal{B}(B \rightarrow K_1(1270)\gamma) < \mathcal{B}(B \rightarrow K_1(1400)\gamma)$ for the negative mixing angles. This is not consistent with the experimental data.

V. DISCUSSIONS AND CONCLUSIONS

As discussed in [9], the discrepancy between theory and experiment for $\mathcal{B}(B \rightarrow K_1(1270, 1400)\gamma)$ is mainly due to the smallness of the relevant form factors. If there is no mixing (i.e., $\theta = 0$), then $F_+^{B \rightarrow K_1(1270)} = F_+^A = 0.256$. This is considerably larger than the previous LCSR result of [11], $F_{+, \text{Safir}}^{B \rightarrow K_1(1270)\gamma} = 0.14 \pm 0.03$. The mixing effects are only 5.7% and -10.6% for $\theta = 37^\circ, 58^\circ$, respectively. In [11], only the asymptotic form of leading twist DA,

$$\phi_\perp^{\text{asy}}(u) = 6u(1-u) , \quad (37)$$

contributes to the sum rule. According to Eq. (31) of [11],

$$F_{+, \text{Safir}}^A(0) = \frac{1}{2} e^{m_B^2/T} \left(\frac{m_b}{m_B^2 f_B} \right) f_A^\perp m_b \int_{u_0}^1 \frac{du}{u} \exp \left[-\frac{m_b^2 + \bar{u} m_A^2}{uT} \right] \phi_\perp^{\text{asy}}(u) . \quad (38)$$

It should be compared with Eq. (27). Eq. (27) improves Eq. (38) in three ways: (1) higher twist DAs are included; (2) non-asymptotic contributions are also included; (3) there is no term proportional to m_A^2 in $F_{+, \text{Safir}}^A(0)$. With the parameter set used in the previous section, we have $F_{+, \text{Safir}}^A(0; s = s_b; T = T_c) = 0.187$. This is larger than the value of $F_{+, \text{Safir}}^{B \rightarrow K_1(1270)\gamma} = 0.14 \pm 0.03$. But if we take the sum rule window of Borel parameter adopted in [11], $F_{+, \text{Safir}}^A(0; s = s_b; T = 7.5 \text{ GeV}^2) = 0.151$, which assures the consistency of the present analysis. We can check how much the new improvements contribute to the form factor. The results are summarized in Table III. One finds that non-asymptotic and higher-twist DA

θ	0°	37°	58°	experiment [2]
$\mathcal{B}(B^0 \rightarrow K_1(1270)^0 \gamma)$	2.81	3.14	2.27	4.28
$\mathcal{B}(B^0 \rightarrow K_1(1400)^0 \gamma)$	0.52	0.14	0.91	< 1.44

TABLE IV: Branching ratios for various mixing angles in units of 10^{-5} .

contributions as well as non-zero mass effects are considerable.

The increase of the form factor will reduce the discrepancy between the theoretical predictions and experimental data [9]. At next-to-leading order of α_s , the branching ratio of $B \rightarrow K_1 \gamma$ is given by [8, 9]

$$\mathcal{B}(B^0 \rightarrow K_1^0 \gamma) = 0.003 \left(1 - \frac{m_{K_1}^2}{m_B^2}\right)^3 \left| F_+^A(0)(-0.385 - i0.014) + (f_A^\perp/\text{GeV})(-0.024 - i0.022) \right|^2. \quad (39)$$

The resulting branching ratios are given in Table IV. The enhancement is significant and the theoretical prediction becomes closer to the experimental data compared to the previous analysis [8], though there is still a gap.

There are a few possibilities to improve further. Firstly, the precisions are different between Eqs. (39) and (27). Eq. (39) contains the hard spectator interactions which appear as a convolution between the jet function and the meson DAs. The DAs contributing to Eq. (39) are leading twist ones and of asymptotic form. It is thus necessary to include higher twist and non-asymptotic contributions in Eq. (39) at the same accuracy as was done in this work. Also, Eq. (27) contains terms proportional to m_A^2 , but Eq. (39) is the result of heavy quark limit. One can easily expect that the next-to-leading order (NLO) of Λ_{QCD}/m_b corrections to the QCDF framework might include the terms of m_A/m_b , but there is no systematics so far. The hard spectator interactions are given by the convolution of hard kernel and meson DAs. Similar non-zero m_A^2 terms will also appear in the axial vector DAs to affect the hard spectator interactions. But this effect is not expected to be large. According to [8], the hard spectator contributions amount to roughly about 5% at the amplitude level.

Secondly, F_+^{A3} could be larger. Actually there is no clue about the size of F_+^{A3} , but it might be that F_+^{A3} is comparable in size to F_+^A , just as in [13]. If this is the case, then the form factor can be enhanced via mixing

$$F_+^{B \rightarrow K_1(1270)} \approx 0.256 \times (\sin \theta + \cos \theta) = 0.35 \sim 0.36, \quad (40)$$

for $\theta = 37^\circ, 58^\circ$, which results in a large branching ratio,

$$\mathcal{B}(B^0 \rightarrow K_1(1270)^0 \gamma) \approx 5.3 \times 10^{-5}. \quad (41)$$

In conclusion, we have calculated $B \rightarrow K_{1B}$ form factor in LCSR. This analysis improves the previous one in a few respects by including higher twist DAs, non-asymptotic contributions, and non-zero m_A^2 terms. The value is rather larger than the previous calculation and that from the quark model result. Larger value is well accommodated to the experimental data. One needs more information about K_{1A} and the mixing angle to reduce theoretical uncertainties. To go beyond the current work, one can include the NLO of α_s which might not be so different from that for $B \rightarrow K^*$ [12]. And the study of $B \rightarrow K_1 \gamma$ at higher accuracy comparable to this work will be necessary.

-
- [1] T. E. Coan *et al.* [CLEO Collaboration], Phys. Rev. Lett. **84**, 5283 (2000) [arXiv:hep-ex/9912057]; S. Nishida *et al.* [Belle Collaboration], Phys. Rev. Lett. **89**, 231801 (2002) [arXiv:hep-ex/0205025]; B. Aubert *et al.* [BABAR Collaboration], Phys. Rev. D **70**, 091105 (2004) [arXiv:hep-ex/0409035].
 - [2] K. Abe *et al.* [BELLE Collaboration], arXiv:hep-ex/0408138; H. Yang *et al.*, Phys. Rev. Lett. **94**, 111802 (2005) [arXiv:hep-ex/0412039].
 - [3] M. Beneke, G. Buchalla, M. Neubert and C. T. Sachrajda, Nucl. Phys. B **591**, 313 (2000) [arXiv:hep-ph/0006124].
 - [4] M. Beneke and T. Feldmann, Nucl. Phys. B **592**, 3 (2001) [arXiv:hep-ph/0008255].
 - [5] M. Beneke, T. Feldmann and D. Seidel, Nucl. Phys. B **612**, 25 (2001) [arXiv:hep-ph/0106067].
 - [6] S. W. Bosch and G. Buchalla, Nucl. Phys. B **621**, 459 (2002) [arXiv:hep-ph/0106081].
 - [7] A. Ali and A. Y. Parkhomenko, Eur. Phys. J. C **23**, 89 (2002) [arXiv:hep-ph/0105302].
 - [8] J. P. Lee, Phys. Rev. D **69**, 114007 (2004) [arXiv:hep-ph/0403034].
 - [9] Y. J. Kwon and J. P. Lee, Phys. Rev. D **71**, 014009 (2005) [arXiv:hep-ph/0409133].
 - [10] M. Jamil Aslam and Riazuddin, Phys. Rev. D **72**, 094019 (2005) [arXiv:hep-ph/0509082]; M. J. Aslam, [arXiv:hep-ph/0604025].
 - [11] A. S. Safir, Eur. Phys. J. directC **3**, 15 (2001) [arXiv:hep-ph/0109232].
 - [12] P. Ball and R. Zwicky, Phys. Rev. D **71**, 014029 (2005) [arXiv:hep-ph/0412079].

- [13] H. Y. Cheng and C. K. Chua, Phys. Rev. D **69**, 094007 (2004) [arXiv:hep-ph/0401141].
- [14] K. C. Yang, JHEP **0510**, 108 (2005) [arXiv:hep-ph/0509337].
- [15] G. Nardulli and T. N. Pham, Phys. Lett. B **623**, 65 (2005) [arXiv:hep-ph/0505048].
- [16] D. Ebert, R. N. Faustov, V. O. Galkin and H. Toki, Phys. Rev. D **64**, 054001 (2001) [arXiv:hep-ph/0104264].
- [17] P. Ball, V. M. Braun, Y. Koike and K. Tanaka, Nucl. Phys. B **529**, 323 (1998) [arXiv:hep-ph/9802299].
- [18] P. Ball and V. M. Braun, Nucl. Phys. B **543**, 201 (1999) [arXiv:hep-ph/9810475].
- [19] S. Eidelman *et al.* [Particle Data Group], Phys. Lett. B **592** (2004) 1.